EBioMedicine 27 (2018) 214–224

Contents lists available at ScienceDirect

EBioMedicine

journal homepage: www.ebiomedicine.com

Research Paper

LDL Receptor Gene-ablated Hamsters: A Rodent Model of Familial Hypercholesterolemia With Dominant Inheritance and Diet-induced Coronary Atherosclerosis

Xin Guo [a,1], Mingming Gao [b,1], Yunan Wang [a,1], Xiao Lin [a], Liu Yang [c], Nathan Cong [a], Xiangbo An [d], Feng Wang [d], Kai Qu [c], Liqing Yu [e], Yuhui Wang [a], Jinjie Wang [a], Haibo Zhu [c], Xunde Xian [f,g,*], George Liu [a,*]

[a] Institute of Cardiovascular Sciences, Key Laboratory of Molecular Cardiovascular Sciences, Ministry of Education, Peking University, Beijing 100191, China
[b] Lipid Metabolism Laboratory, Institute of Basic Medicine, Hebei Medical University, Shijiazhuang, China
[c] State Key Laboratory of Bioactive Substance, Function of Natural Medicines & Ministry of Health Key Laboratory of Biosynthesis of Natural Products, Chinese Academy of Medical Sciences, Peking Union Medical College, Beijing, China
[d] Department of Interventional Radiology, First Affiliated Hospital of Dalian Medical University, Dalian 110611, China
[e] Center for Molecular and Translational Medicine, Institute for Biomedical Sciences, Georgia State University, Atlanta, GA 30303, USA
[f] Department of Molecular Genetics, UT Southwestern Medical Center, Dallas, TX 75390, USA
[g] Department of Biochemistry and Molecular Biology, College of Basic Medicine, Hebei Medical University, Shijiazhuang, China

ARTICLE INFO

Article history:
Received 8 September 2017
Received in revised form 12 December 2017
Accepted 12 December 2017
Available online 15 December 2017

Keywords:
LDL receptor
Golden Syrian hamster
Hyperlipidemia
Atherosclerosis
CRISPR/Cas9

ABSTRACT

Familial hypercholesterolemia (FH) is an autosomal dominant genetic disease caused mainly by LDL receptor (*Ldlr*) gene mutations. Unlike FH patients, heterozygous *Ldlr* knockout (KO) mice do not show a dominant FH trait. Hamsters, like humans, have the cholesteryl ester transfer protein, intestine-only ApoB editing and low hepatic cholesterol synthesis. Here, we generated *Ldlr*-ablated hamsters using CRISPR/Cas9 technology. Homozygous *Ldlr* KO hamsters on a chow diet developed hypercholesterolemia with LDL as the dominant lipoprotein and spontaneous atherosclerosis. On a high-cholesterol/high-fat (HCHF) diet, these animals exhibited severe hyperlipidemia and atherosclerotic lesions in the aorta and coronary arteries. Moreover, the heterozygous *Ldlr* KO hamsters on a short-term HCHF diet also had overt hypercholesterolemia, which could be effectively ameliorated with several lipid-lowering drugs. Importantly, heterozygotes on 3-month HCHF diets developed accelerated lesions in the aortas and coronary arteries.

Our findings demonstrate that the *Ldlr* KO hamster is an animal model of choice for human FH and has great potential in translational research of hyperlipidemia and coronary heart disease.

1. Introduction

Familial hypercholesterolemia (FH) is a major form of hypercholesterolemia characterized by elevated blood cholesterol levels due to delayed clearance of plasma low density lipoproteins (LDLs), leading to the early onset of cardiovascular and cerebrovascular diseases (Hobbs et al. 1992). FH pathogenesis hinges upon loss-of-function mutations in the *Ldlr* gene, which interacts with additional genetic and environmental factors. Significant resources have been allocated to FH research, including animal models based on various species in which human FH can be simulated by deleting the *Ldlr* gene with current genetic engineering techniques (Ishibashi et al. 1993; Li et al. 2016). Among these species, mice have been the most popular because of their small size, rapid breeding and low cost. However, lipid metabolism in mice differs from that in humans with respect to 1) the absence of cholesteryl ester transfer protein (CETP), 2) the presence of both intestinal and hepatic ApoB editing activity, and 3) the high hepatic expression of *Ldlr* mRNA. Thus, mice are "HDL predominant" because they lack CETP-mediated cholesterol transfer from HDL to VLDL and display a fast clearance of ApoB48-containing lipoproteins resulting from additional hepatic ApoB editing. Despite the current widespread use of *Apoe* KO and *Ldlr* KO mice to mimic human atherosclerosis, obvious differences in murine genetic and metabolic profiles limit their further applications

Abbreviations: ApoB, apolipoprotein B; ApoE, Apolipoprotein E; CETP, cholesteryl ester transfer protein; CAD, coronary artery disease; CD, chow diet; CHD, cardiovascular heart diseases; CRISPR/Cas9, clustered regularly interspaced short palindromic repeats and CRISPR-associated protein 9; FH, familial hypercholesterolemia; HDL, high density lipoprotein; HCHF, high cholesterol high fat; HeFH, heterozygous familial hypercholesterolemia; HoFH, homozygous familial hypercholesterolemia; KO, knockout; LDL, low density lipoprotein; LDLR, low density lipoprotein receptor; LPL, lipoprotein lipase; PCSK9, proprotein convertase subtilisin/kexin type 9; VLDL, very low density lipoprotein.

* Corresponding authors.
E-mail addresses: xunde.xian@utsouthwestern.edu (X. Xian), georgeliu@bjmu.edu.cn (G. Liu).

[1] These authors contributed equally to this work.

https://doi.org/10.1016/j.ebiom.2017.12.013

(Getz and Reardon 2006). In contrast, golden Syrian hamsters are small rodents that exhibit many features that are similar to those of humans, including lipoprotein profile, high plasma CETP levels, and ApoB editing only in the intestine (Reaves et al. 2000). In particular, hamsters are susceptible to high-fat diet-induced combined hyperlipidemia (Haidari et al. 2002). In addition, one study (Bjorklund et al. 2014) recently used AAV-mediated hepatic gene delivery to introduce a PCSK9 gain-of-function mutant gene (rAAV8-D377Y-mPCSK9) to hamsters, and their results revealed hypercholesterolemia and atherosclerosis that were similar to those observed in mice when both species were fed a western-type diet. However, this non-germline approach is questionable because although >95% of hepatic LDLR is reduced in the rAAV8-D377Y-mPCSK9 model, the plasma cholesterol levels are not as high as those in the *Ldlr*−/− model, indicating that LDLR from extrahepatic or other tissues can contribute to this cholesterol-lowering effect. Additionally, a systemic review of the literature reveals that genes associated with atherosclerosis in mice are scarcely confirmed in human diseases with common genetic variants, suggesting that the use of gene-modified mouse models is insufficient to fully understand the potential pathogenesis underlying atherosclerosis (Pasterkamp et al. 2016). Furthermore, due to the technical limitations of hamster embryo manipulation, genetically modified hamster models have not been generated to study the human hereditary hyperlipidemia pathogenesis and experimental interventions.

Recently, we achieved a technological breakthrough in hamster embryo manipulation and successfully generated the genetically engineered hamster (Gao et al. 2014). Herein, we report the generation of *Ldlr* knockout hamsters using the CRISPR/CAS9 gene editing technique (Cong et al. 2013) and show that this model manifests pathological phenotypes similar to those of humans with respect to autosomal inherited hypercholesterolemia and coronary atherosclerotic lesions.

2. Materials and Methods

2.1. Hamster Model

Golden Syrian hamsters were purchased from Vital River Laboratories (Beijing, China) and maintained in an air-conditioned room with a 14/10-hour light/dark cycle. For HCHF diet intervention experiments, 8–10 weeks old animals were fed with HCHF for the indicated time points. All experiments were monitored according to the principles of laboratory animal care (NIH publication no.85Y23, revised 1996) and approved by the Animal Care and Use Committee of the Peking university health science center (LA2010-059).

2.2. sgRNA Design

The sgRNA targeting sites of interest were identified by searching for the GG(N)18NGG motifs in the DNA sense or antisense strands. The specificity of the sgRNA target sites was analyzed according to the basic local alignment search tool (BLAST) applied to the golden Syrian hamster genome. The targeting sequence of the *Ldlr* gRNAs was gaaatgcatcgccagcaag[*tgg*].

2.3. Production of sgRNA and Cas9 mRNA

The sgRNA template was amplified by PCR. In a 50-μL PCR volume, the reaction comprised a unique oligonucleotide (CRISPRF) harboring the T7 polymerase binding site; the sgRNA target sequence, GG(N)18; and a common oligonucleotide (sgRNAR) encoding the remainder. The reaction was performed on a thermal cycler (98 °C for 30 s and 35 cycles of 98 °C for 10 s, 60 °C for 30 s, and 72 °C for 15 s, followed by 72 °C for 10 min and 4 °C for ∞), and the PCR products were purified using a Gel DNA Extraction Kit (TAKARA) and by phenol chloroform extraction, with subsequent isopropanol precipitation. The sgRNA template was transcribed using Megascript T7 Kit (Ambion) in vitro, purified with the MEGAclear Kit (Ambion), diluted in RNase-free water to a final concentration at 200 ng/μL and stored at −80 °C for future use.

The PXT7 construct carrying a humanized cas9 cDNA was used as the DNA template for the amplification of the cas9 coding sequence. The PXT7 vector was linearized with *Xba*I and purified by ethanol precipitation. Cas9 mRNA was transcribed using linearized template DNA with the mMESSAGE mMACHINE T7 kit (Ambion) and purified by phenol chloroform extraction and isopropanol precipitation. Cas9 mRNA was diluted into RNase-free water to a final concentration at 500 ng/μL and stored at −80 °C for future use.

2.4. Microinjection

Microinjections were performed under a microscope with red filters. M2 medium covered by mineral oil was used as the injection medium. sgRNA (20 ng/μL) and cas9 mRNA (50 ng/μL) were co-injected into the cytoplasms of fertilized eggs with well-recognized pronuclei in M2 medium (Sigma-Aldrich, St. Louis, MO, USA). The injected zygotes were cultured in HECM-10 medium at 37.5 °C under 10% CO_2 for 30 min. Thereafter, the injected embryos with normal morphology were transferred into each oviduct (approximately 15 embryos per oviduct) through the fimbriae of the female recipients; the females were naturally mated with male litters for 24 h before the transfer, as described previously (Fan et al. 2014).

2.5. Genotyping

Genomic DNA was extracted from the toes into 200 μL of squishing buffer (10 mM Tris-HCl, 1 mM EDTA, 25 mM NaCl, 500 mg/mL proteinase K, pH 8.2) and incubated at 55 °C for 12 h, followed by inactivation at 95 °C for 10 min. The targeted fragments were amplified from the extracted DNA, and mutations were identified by Sanger sequencing. The *Ldlr* KO hamsters were genotyped with primers *Ldlr*-F (5′-CGGCCC AGATGTCAATAT-3′) and *Ldlr*-R (5′-GTGAAACCCTCCAAACCC-3′).

Furthermore, the amplified products were cloned into the pEASY-T1 vector (Transgen Biotech). After transformation of the reactions, the targeted DNAs isolated from single clones were sequenced.

2.6. Off-target Analysis

Potential off-target analysis was based on the rules indicating that sequences matching the final 12 nt of the target sequence and PAM sequence may cause off-target effects (Cong et al. 2013). Potential off-target fragments were amplified from the extracted DNA and identified by Sanger sequencing.

2.7. Plasma Lipids, Oral Fat Load, VLDL Secretion and LPL Activity Assay

The total plasma cholesterol (TC) and triglyceride (TG) levels were determined enzymatically using commercially available kits (Sigma). After ApoB-containing lipoproteins were precipitated with 20% polyethylene glycol solution, HDL cholesterol (HDL-c) was measured with the aforementioned kit. Fast-Protein Liquid Chromatography (FPLC) of plasma lipoproteins was performed from pooled plasma aliquots (250 μL) and applied to Tricorn high-performance Superose S-6 10/300GL columns using a fast-protein liquid chromatography system (Amersham Biosciences), followed by elution with PBS at a constant flow rate of 0.25 mL/min. Eluted fractions (500 μL per fraction) were assessed for triglyceride and cholesterol concentrations using the same TG and cholesterol kits.

In the oral fat load assay, 8–10 weeks old male hamsters on chow diet were fasted for 12 h and then gavaged with olive oil (10 mL/kg body weight). Plasma was collected for TG measurement at the indicated time points (0 h, 0.5 h, 1 h, 2 h, 3 h, 4 h, and 8 h) after gavage.

After male hamster on the indicated diets for two weeks were fasted for 12 h, VLDL secretion was evaluated by ip injection with 7.5% Poloxamer (Sigma) at 1500 mg/kg. Blood was collected at different time points after the injection (Millar et al. 2005). Plasma TG was measured as described above.

To assess the post-heparin plasma LPL activity in chow diet-fed male hamsters, blood was drawn 10 min after iv injection of 100 U/kg heparin, and the plasma was isolated at 4 °C. LPL catalytic activity was measured and expressed as micromole/mL/min of released FFA as described previously (DI Filippo et al. 2014).

2.8. Pathological Analysis

8–10 weeks old hamsters fed indicated diets for 12 weeks, were sacrificed and then perfused with 20 mL of 0.01 M cold phosphate-buffered solution through the left ventricle. The hearts were harvested, fixed in a 4% paraformaldehyde solution for 1 week and stored in a 20% sucrose solution overnight. After fixation, the hearts were embedded in OCT, cross-sectioned (7 μm per slice) and stored at −70 °C for future use. Lipid deposition in the whole aorta (en face) and aortic root sections was examined by staining with a 0.3% Oil Red O solution (Sigma-Aldrich, USA) for 30 min at room temperature, following by rinsing with 60% isopropanol and distilled water. For lesion assessment in the whole aorta or individual regions, we defined 3 segments as follow: 1) the aortic arch: aortic root to 3 mm below the left subclavian; 2) the thoracic aorta: the region between the end of the arch and the last intercostal branch; 3) the abdominal aorta: the region between the end of thoracic aorta segment to the iliac bifurcation. To characterize the atherosclerotic lesions, Immunohistochemistry of CD68, VCAM-1 and SMA was performed using cryo-sections of the hearts with a primary CD68 antibody (1:100 rabbit polyclonal IgG; BA3638, BOSTER), VCAM-1 antibody (1:100 rabbit polyclonal IgG; BA3840, BOSTER) and α-SMA antibody (1:100 rabbit polyclonal IgG; A03744, BOSTER). The slices were then incubated with appropriate biotinylated second antibodies (1:200, ABC Vectastain; Vector Laboratories, Burlingame, CA, USA) in 2% normal blocking serum and visualized using 3, 3′-diaminobenzidine (DAB, Vectastain; Vector Laboratories). Coronary arteries were visually scored according to the severity of the stenosis as follow with modification: unaffected (0%), minor occlusion (<5%) and partial occlusion (5–20%). The hearts at the level of papillary muscle were embedded in paraffin and cross-sectioned (5 μm per slice). Sirius red staining was performed to assess fibrosis in the myocardium.

2.9. Quantification and Statistical Analysis

Comparisons were analyzed by Student's *t*-test or two-way ANOVA. VLDL secretion was analyzed by linear regression. Pearson's correlation was used to analyze two independent variables. A p value < 0.05 was considered to indicate statistical significance. All data were expressed as the mean ± SEM.

3. Results

3.1. Generation of Ldlr Knockout Hamsters Using the CRISPR/Cas9 System

To generate *Ldlr* KO hamsters, we designed a gRNA targeting exon 2 of the hamster *Ldlr* gene (Fig. 1a). The gRNA and Cas9 mRNA were microinjected into the cytoplasms of 120 fertilized eggs, and the fertilized eggs were then transferred into 4 female hamsters, leading to the birth of 16 offspring. DNA sequencing of the PCR products from the targeted region showed that 2 of the offspring, founders 1 and 2, had mutations in the targeted site and that there were no off-target mutants (data not shown). Of these two *Ldlr* mutant lines, founder 1 was a genetic mosaic carrying 12, 10, 14 and 5 nucleotide deletions, whereas founder 2 was a compound heterozygous mutant carrying a deletion of 194 nucleotides and a transition of AG to GC (Fig. 1b). All mutations could undergo germline transmission. To confirm that the *Ldlr* gene had been successfully targeted, we performed PCR and Western blots. Genotyping by PCR using tail genomic DNA easily detected the 194-nucleotide deletion (Δ194) in both the heterozygous and homozygous F2 offspring (Fig. 1c). The Western blots of the liver homogenates showed that the LDLR protein was undetectable in the homozygotes and was only approximately 50% present in the heterozygotes compared to the WT hamsters (Fig. 1d and e).

3.2. Characteristics of Plasma Lipids and Lipoproteins in Ldlr Knockout Hamsters

When the 2 founders were crossed with wild-type (WT) hamsters, 6 different genotypes of heterozygous progeny were obtained. Two lines of the *Ldlr* mutant hamsters (Δ194 and Δ10) were further bred to obtain the offspring in our present study. Since *Ldlr* is a key determinant of plasma lipids, we analyzed and characterized the lipid profiles of the WT and *Ldlr* KO hamsters. As shown in Table 1, compared to the WT hamsters (147.5 ± 4.56 mg/dL), the plasma TC levels in the Δ194 and Δ10 *Ldlr* heterozygote hamsters at 2 months of age were significantly elevated to 230.1 ± 9.95 mg/dL and 219.1 ± 5.54 mg/dL, respectively. Additionally, we also found increased plasma TG in the homozygotes of both the Δ194 (490.4 ± 21.17 mg/dL) and Δ10 (504.6 ± 20.61 mg/dL) genotypes, compared to the control animals (169.7 ± 12.42 mg/dL), but no difference was observed between the Δ194 and Δ10 heterozygotes and the WT hamsters (197.7 ± 14.42 mg/dL, 221.1 ± 12.72 mg/dL and 169.7 ± 12.42 mg/dL, respectively). Surprisingly, no significant changes in the plasma HDL-C levels were observed between any genotype groups. Next, when we investigated whether the lipid levels were sex-dependent in our animals, we found that there were no sex discrepancies in plasma cholesterol, TG or HDL-C within the same genotype for either the heterozygotes or homozygotes (Fig. 2a, b and c). Because the two *Ldlr* mutant lines presented with similar plasma lipid levels, only the animals from the Δ194 line were chosen for subsequent experiments in our study.

To better understand the plasma cholesterol distribution in different species on chow diet, we performed FPLC to analyze lipoprotein fractionation from male WT, heterozygous and homozygous hamsters and compared the results to those counterparts. As expected, the FPLC results revealed a distinct LDL peak in the WT hamsters that was more pronounced in the heterozygous *Ldlr* (*Ldlr*+/−) hamsters (Fig. 2d, right panel), a characteristic phenotype that was similar to humans (Fig. 2d, left panel). Interestingly, the homozygous *Ldlr* (*Ldlr*−/−) mutant hamsters displayed markedly elevated cholesterol levels in the LDL fraction. In the meantime, we also observed a significant increase in VLDL-C in the *Ldlr*−/− hamsters. Unlike humans and hamsters, the *Ldlr*−/− mice only exhibited a moderate increase in the LDL fraction (Fig. 2d, middle panel). In addition, compared to the WT controls, we found that the *Ldlr*+/− hamsters showed a modest increase in TG in the VLDL fraction; however, the *Ldlr*−/− hamsters exhibited markedly elevated TG in the VLDL fraction (Supplemental Fig. 1), suggesting that the metabolisms of both cholesterol and triglycerides in lipoproteins were impaired in the *Ldlr*-ablated hamsters in a gene dose-dependent manner.

To assess if the distinct VLDL fraction and increased TG in the *Ldlr*−/− hamsters were attributable to the impaired clearance of circulating lipoprotein from the plasma or to the over-production of VLDL by the liver, we performed assessments of the oral fat load and of hepatic VLDL secretion. In the oral fat load experiment, after 12 h of fasting, 8–10 weeks old male hamsters were given olive oil at a dose of 10 mL/kg body weight, and blood was collected for plasma TG measurements at indicated time points. As shown in Fig. 2e, compared to the WT controls, the TG levels were significantly increased in both the *Ldlr*+/− and *Ldlr*−/− hamsters beginning at 2 h after gavage, and the *Ldlr*−/− hamsters displayed much higher TG levels during the whole experimental period, indicating that lipoprotein clearance was delayed in

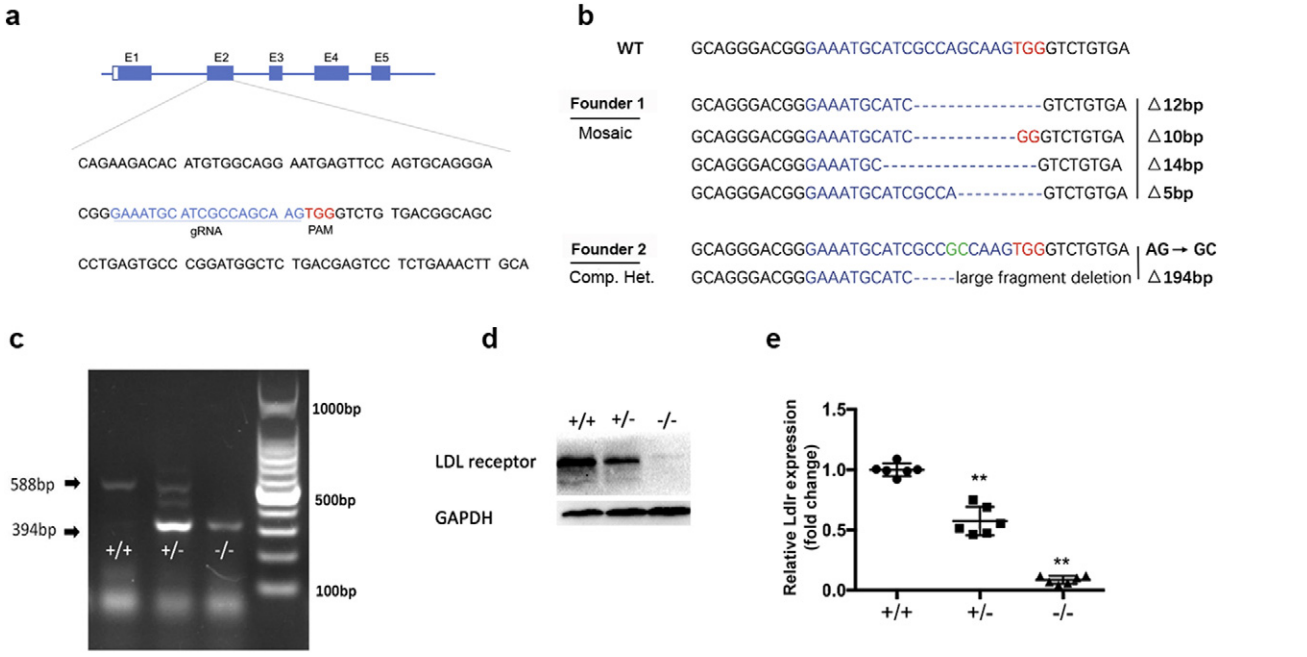

Fig. 1. Generation of Ldlr knockout hamster model. (a) Schematic diagram of the gRNA targeting sites at the Ldlr loci. The gRNA target sequence is labeled in blue. The letters in red indicate the protospacer adjacent motif (PAM). (b) Sequencing of the targeted site in the two mutant founders. The gRNA-targeted sequence is labeled in blue, and the PAM sequence is in red. GC in green from founder 2 means two point mutations. On the right side of each allele, the type of mutation and sizes of deletions (Δ) are indicated. (c) PCR analysis was performed using tail genomic DNA from WT (+/+), heterozygote (+/−) and homozygote (−/−) with the Δ194 deletion. (d) Representative Western blot of hepatic LDLR from the indicated hamsters described in (c). (e) Quantitative analysis of hepatic LDLR protein levels in the 8–10 weeks old male hamsters with different genotypes. Data are the mean ± SEM from 6 animals. All values are expressed as the mean ± SEM. ** and *** denote $p < 0.01$ and $p < 0.001$, respectively, vs WT.

the *Ldlr*-mutant hamsters. Next, VLDL secretion was evaluated by investigating the change in plasma TG during a 4-hour course after blocking lipoprotein lipase (LPL) activity via ip injection of Poloxamer (1500 mg/kg), an LPL inhibitor. As shown in Fig. 2f, the secretion rate of VLDL-TG was not altered in these three genotypes. Furthermore, we measured the activity of LPL, which is responsible for the hydrolysis of circulating TG, and no differences were observed in the 8–10 weeks old male WT and *Ldlr* −/− hamsters (Fig. 2g). Taken together, these data suggest that elevated TG levels are attributable to the impaired receptor-mediated clearance of large TG-rich lipoproteins in *Ldlr* mutant hamsters and that these levels are also dependent on the copy number of *Ldlr* gene.

3.3. Response of Plasma Lipids to a High-Cholesterol/High-Fat Diet and Hypolipidemic Agents

Due to the nature of autosomal dominant inheritance, most FH patients with heterozygous *Ldlr* gene mutations develop premature coronary artery disease (CAD). Although WT hamsters have been reported to be sensitive to a high-fat diet, it would be intriguing to know whether the loss of only one copy of the *Ldlr* gene would further predispose hamsters to diet-induced hyperlipidemia, as observed in FH patients. To test our hypothesis, 8–10 weeks old WT and *Ldlr* +/− hamsters were subjected to a high-cholesterol/high-fat (HCHF, 0.5% Cholesterol and 15% lard) diet for 2 weeks, and parallel comparisons were made between WT and *Ldlr* +/− mice. On the chow diet, both the *Ldlr* +/− hamsters and mice had slightly higher TC levels than their corresponding WT controls. However, after the HCHF challenge for 2 weeks, the TC levels in the WT hamsters increased by 4-fold from 131.6 ± 11.6 to 513.3 ± 35.5 mg/dL (Fig. 3a). Striking changes were observed in the *Ldlr* +/− hamsters; the plasma TC levels of the *Ldlr* +/− hamsters were >10-fold higher than those of the WT hamsters (170.8 ± 8.2 to 2078 ± 163.9 mg/dL) (Fig. 3a). Hence, the *Ldlr* +/− hamsters were more susceptible to diet-induced hyperlipidemia. Analysis of the cholesterol distribution by FPLC showed dramatic increases in LDL and VLDL fractions in the *Ldlr* +/− hamsters that were fed HCHF for only 2 weeks compared to the WT controls (Fig. 3b, right panel). However, there were no significant changes in the plasma cholesterol levels and cholesterol distribution between the WT and *Ldlr* +/− mice on the HCHF diet for 2 weeks (Fig. 3b, left panel). Interestingly, in the setting of the 2-week HCHF diet, hamsters displayed marked elevation of plasma lipids (the TC and TG levels were 3099.1 ± 381.2 and 5898.3 ± 892.5 mg/dL, respectively for the *Ldlr* −/− hamsters; 1089.9 ± 112.6 and 1296.1 ± 445.0 mg/dL, respectively for the *Ldlr* +/− hamsters, and 632.9 ± 120.8 and 553.2 ± 199.6 mg/dL, respectively for the WT hamsters). Moreover, when compared to WT and *Ldlr* +/− animals,

Table 1
Analysis of plasma lipids in indicated hamsters on the chow diet.

(mg/dL)	WT	*Ldlr* +/−		*Ldlr* −/−	
	(N = 28)	Δ194bp (N = 28)	Δ10bp (N = 28)	Δ194bp (N = 16)	Δ10bp (N = 16)
TC	147.5 ± 4.56	230.1 ± 9.95**	219.1 ± 5.14**	735.9 ± 30.02**,##	722.2 ± 17.64**,##
TG	169.7 ± 12.42	197.7 ± 14.42	221.1 ± 12.72	490.4 ± 21.17**,##	504.6 ± 20.61**,##
HDL-C	92.2 ± 4.19	92.4 ± 3.77	95.9 ± 3.94	94.9 ± 4.55	99.0 ± 4.69

** denote $p < 0.01$ vs WT.
denote $p < 0.01$ vs *Ldlr* +/−.

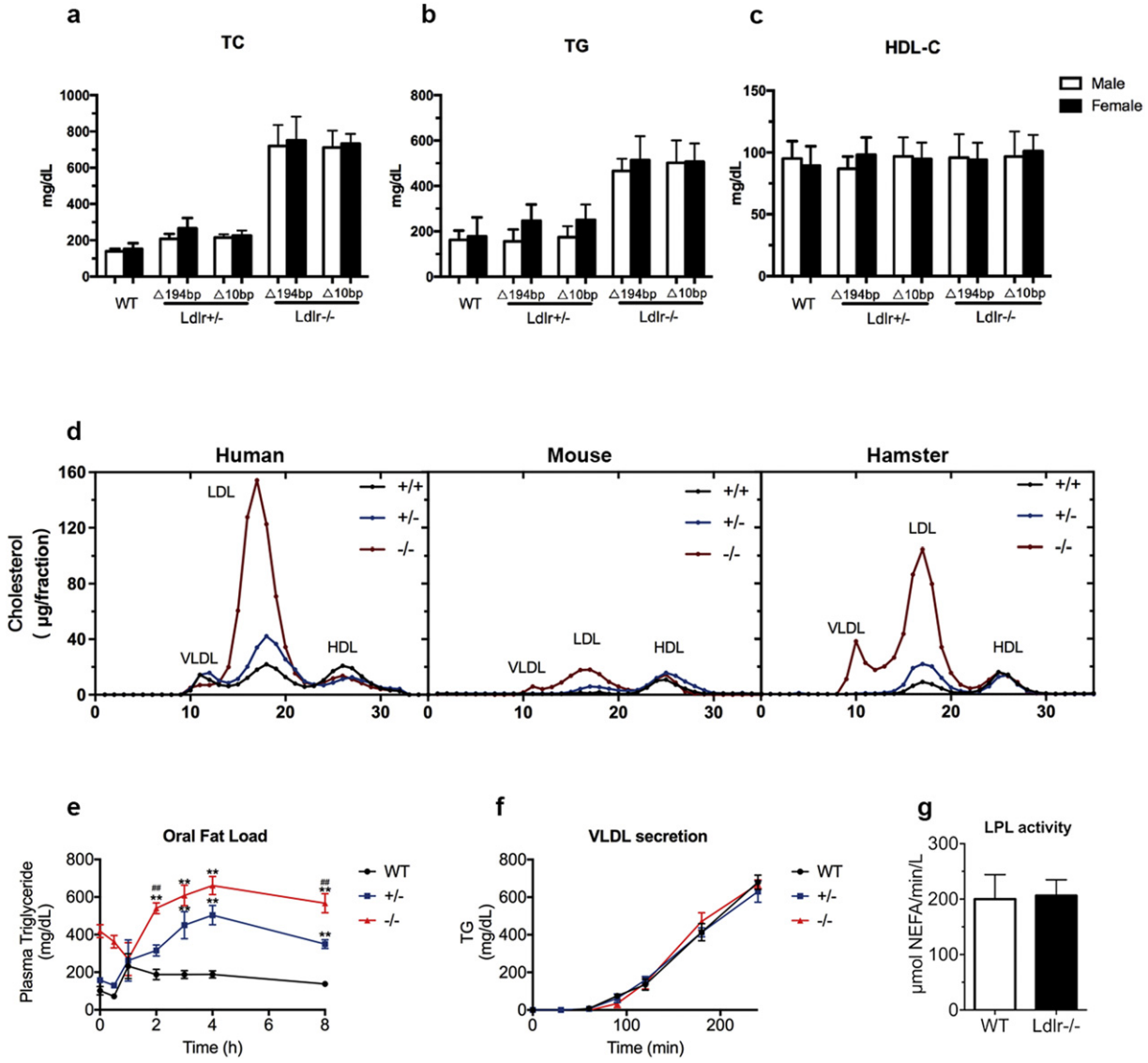

Fig. 2. Analysis of plasma lipids, oral fat load, VLDL secretion and post-heparin plasma LPL activity. (a–c) Plasma TC, TG and HDL-C of the chow diet-fed male hamsters at 8–10 weeks of age (n = 8 to 16 per group). (d) FPLC analysis of the lipoprotein distribution in pooled plasma from normal and *Ldlr*-mutated humans, mice and hamsters on a regular chow diet (5–6 animals, mixed sex). (e) Oral fat load was assessed in 8–10 weeks old male hamsters on a regular chow diet that were fasted for 12 h and gavaged with olive oil at 10 mL/kg body weight. Plasma was collected at different time points for TG measurements (n = 6 per group). (f) VLDL secretion was conducted in the 12-h fasted 8–10 weeks old male animals on a regular chow diet by injecting 1500 mg/kg poloxamer. Plasma was collected at the indicated time points for TG assays (n = 6 per genotype). (g) Post-heparin plasma LPL activity in the 8–10 weeks old WT and *Ldlr*−/− hamsters with chow diet feeding. LPL activity was measured using blood on ice that was collected10 min after an intravenous injection of 100 U/kg heparin (n = 6 per genotype). All data are expressed as the mean ± SEM. ** denotes $p < 0.01$ vs WT hamsters. ## denotes $p < 0.01$ vs *Ldlr*+/− hamsters.

Ldlr−/− hamsters had severe hyperlipidemia, but did not display accumulated TG in circulation after the P407 injection, indicating that hepatic VLDL secretion was completely blunted in the HCHF diet-fed *Ldlr*−/− hamsters (Supplemental Fig. 2).

To evaluate whether the *Ldlr*+/− hamsters responded to treatments with different lipid-lowering agents, we treated 8–10 weeks old hamsters on the HCHF diet for 2 weeks with Rosuvastatin (2 mg/kg), Ezetimibe (2 mg/kg) and Fenofibrate (100 mg/kg), which are three common clinically available lipid-lowering agents. Oral administration of these agents resulted in a marked decrease in plasma TC and TG in the hyperlipidemic *Ldlr*+/− hamsters, with Ezetimibe being most effective (Fig. 3c). Ezetimibe also had a highly potent effect toward lowering the TC levels in the WT hamsters on the HCHF diet; however, Rosuvastatin and Fenofibrate at the chosen dose had little to no effect. The FPLC data also demonstrated that, similar to the plasma total cholesterol levels, Ezetimibe significantly reduced the cholesterol concentrations in the VLDL/LDL fractions in the HCHF-fed animals (Fig. 3d).

3.4. Aortic and Coronary Atherosclerotic Lesion Development in Ldlr +/− Hamsters

Atherosclerosis is the major consequence of hypercholesterolemia both clinically and in research animal models. Attempts were therefore made to explore whether *Ldlr*+/− hamsters on the HCHF diet developed accelerated atherosclerosis. When 8–10 weeks old WT and *Ldlr*+/− hamsters were challenged with the HCHF diet for 12 weeks, we found that the lack of one copy of the *Ldlr* gene in hamsters elicited severe hypercholesterolemia with TC levels higher than 2000 mg/dL beginning at 2 weeks, which was consistent with the findings of the drug intervention (Fig. 4a). The TG levels in the *Ldlr*+/− hamsters were also significantly increased after being fed the HCHF diet for 4 weeks (Fig. 4b). After 12 weeks of the HCHF diet, Oil Red O staining of the atherosclerotic lesions in the aorta revealed significantly increased lesion areas in the whole aorta and aortic roots (Fig. 4c–g) in *Ldlr*+/− hamsters compared to the WT controls (Fig. 4h and i). To confirm the

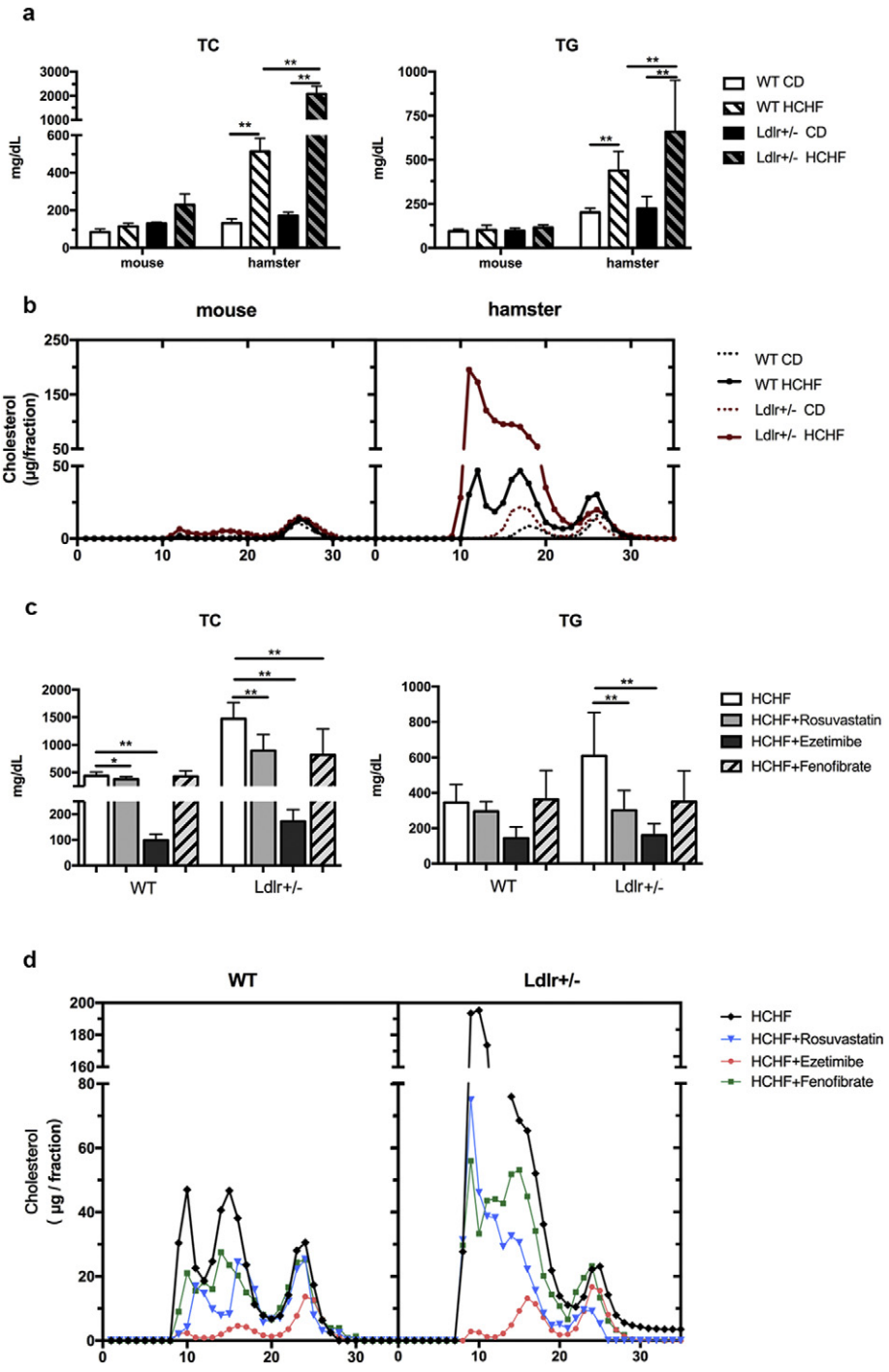

Fig. 3. Response of plasma total cholesterol and lipoprotein profile in WT and *Ldlr*+/− mice and hamsters to short-term feeding of the HCHF diet and effect of oral rosuvastatin, ezetimibe and fenofibrate on plasma lipids. (a) Analysis of plasma total cholesterol levels in different male animals on the CD or HCHF diet for 2 weeks (n = 6 per group). ** denotes $p < 0.01$. (b) Cholesterol distribution in different lipoprotein fractions by FPLC in different animals on the indicated diet for 2 weeks (pooled plasma from 5 to 6 animals per group). (c) Plasma total cholesterol levels were monitored in WT and *Ldlr*+/− hamsters on the HCHF diet with oral administration of 3 common lipid-lowering medications, namely, Rosuvastatin (2 mg/kg), Ezetimibe (2 mg/kg) and Fenofibrate (100 mg/kg) (n = 10 per group). * and ** denote $p < 0.05$ and <0.01, respectively. (d) The cholesterol concentrations in the different FPLC fractions were analyzed in the indicated animals described above in (c). All values are expressed the mean ± SEM.

content in the lesions, we performed immunohistochemical staining and found that more positive staining for CD68 (a macrophage maker) and VCAM1 (an inflammatory marker) was observed in the lesion areas (Fig. 4j). However, the expression levels of SMA, a marker of smooth muscle cells (SMCs), were identical between both genotypes, indicating that macrophages, but not SMCs, were the major drivers of the pathogenesis underlying atherosclerosis. In addition, it was noted that the *Ldlr*+/− hamsters also exhibited atherosclerotic lesions in the circumflex branches of the left coronary artery (LCA) (Fig. 4k). The semi-quantitative data demonstrated that the coronary arteries were not affected in the WT controls; however, although 52% of the coronary arteries were unaffected in the *Ldlr*+/− group, 26% of the coronary arteries showed lesions with <5% occlusion (minor occlusion), and 21% of the coronary arteries had occluded lesions between 5% and 20% (partial occlusion) (Fig. 4l).

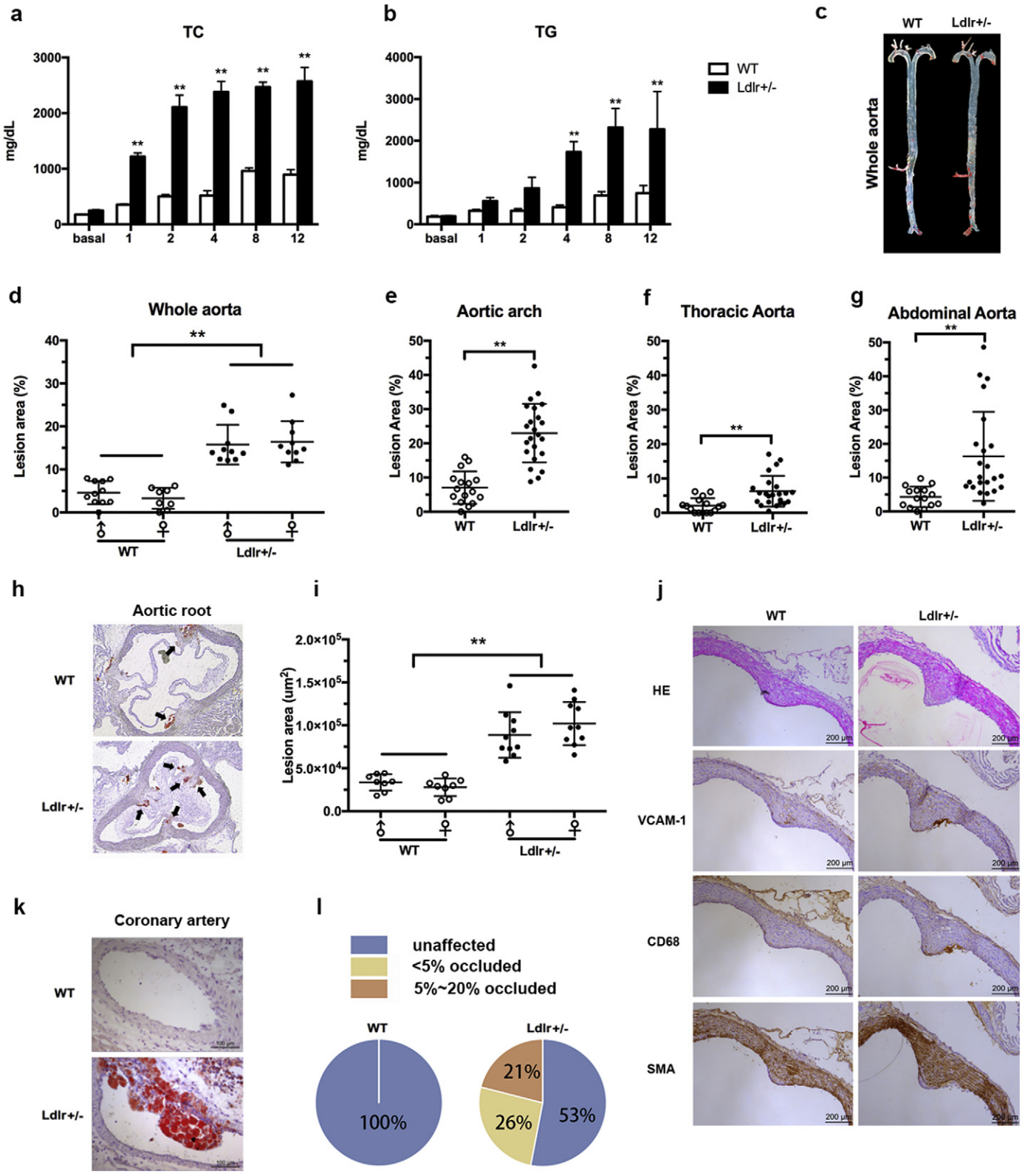

Fig. 4. Analysis of plasma lipids and aortic and coronary atherosclerotic lesions in the WT and *Ldlr*+/− hamsters on the HCHF diet for 12 Weeks. (a and b) Plasma TC and TG were measured at the indicated time points in WT (n = 16) and *Ldlr*+/− (n = 20) hamsters on the HCHF diet for 12 weeks. The lesion size in the whole aorta was quantified in the mixed-sex hamsters. (c) Representative en face image of the whole aorta in the WT and *Ldlr*+/− hamster. (d–g) The lesion sizes in the whole aorta (D), aortic arch (e), thoracic aorta (f) and abdominal aorta (g) were quantified in the mixed-sex hamsters. (h) Representative Oil Red O staining of the aortic root in the WT and *Ldlr*+/− hamsters. (i) Lesion areas in the aortic root were quantified (WT, n = 16; *Ldlr*+/−, n = 20). ** denotes $p < 0.01$. (j) Immunohistochemical analysis of the atherosclerotic lesions in the WT and *Ldlr*+/− hamsters after 12 weeks on the HCHF diet. Representative staining of HE, CD68, VCAM1 and SMA in the lesion from the aortic root. (k) Representative image of the coronary atherosclerotic lesion in the WT and *Ldlr*+/− hamsters. (l) Semi-quantitative measurements of lesions in the coronary arteries of the WT (n = 16) and *Ldlr*+/− hamsters (n = 20). The arrows indicate positive staining. The black arrows indicate Oil Red O positive staining. Scale bar = 200 μm. All values are expressed the mean ± SEM.

3.5. Spontaneous Atherosclerosis and Diet-Induced Coronary Artery Disease in *Ldlr* −/− Hamsters

Because hyperlipidemia is a major risk factor for atherosclerosis and the *Ldlr* −/− hamsters showed elevated TC and TG levels while on the chow diet, we investigated whether the *Ldlr* −/− hamster model was sensitive to atherogenesis. As shown in Fig. 5, the male *Ldlr* −/− hamsters at 12 months had undetectable lesions in both the whole aorta and aortic root. However, the aged male *Ldlr* −/− hamsters at 18 months had significant development of atherosclerosis compared to those at 12 months, and this phenotype was also observed in the aged *Ldlr* −/− mice on the chow diet. In addition to spontaneous atherosclerosis, homozygous FH patients without any treatment die from premature coronary artery disease (CAD), but no mortality has been reported for homozygous *Ldlr* KO mice. Moreover, a special diet containing 3% cholesterol and 20% butter was used to demonstrate that this treatment induced coronary atherosclerosis in WT hamsters (Sima et al. 1990). To study CAD in our model, we fed 8–10 weeks male *Ldlr* −/− hamsters the HCHF diet for 12 weeks. As shown in Fig. 6a, the *Ldlr* −/− hamsters had severe hypercholesterolemia over 4000 mg/dL at 4 weeks and approximately 6000 mg/dL at 8 to 12 weeks, and these levels were much higher than those of the WT controls on the 3% high-cholesterol diet. In the meantime, both the WT and *Ldlr* −/− hamsters also exhibited markedly increased TG levels (Fig. 6b). The survival rate demonstrated that the *Ldlr* −/− hamsters on the HCHF diet started to die on day 14 and that half of the animals died on day 30 (Fig. 6c). This remarkable finding drove us to analyze the pathological changes in the cardiovascular system. Oil Red O staining revealed that the HCHF-fed *Ldlr* −/− hamsters displayed advanced atherosclerosis in the both aorta and coronary arteries (Fig. 6d–f). We also observed severe fibrosis in the myocardium using Sirius red staining, suggesting that myocardial infarction could be a leading cause of death in *Ldlr* −/− hamsters (Fig. 6g). It was noted that dietary treatment with 3% cholesterol did not elicit severe atherosclerotic lesions in the aortas and did not elicit lesions in the coronary arteries of the WT hamsters. Collectively, these data demonstrate that the *Ldlr* KO hamster is a human-like animal model of cardiovascular disease.

4. Discussion

In the present study, we have generated a human-like animal model of familial hypercholesterolemia using the CRISPR/Cas9 editing system to delete the *Ldlr* gene in hamsters. In striking contrast to mice, the loss of one copy of the *Ldlr* gene in hamsters results in a modest increase in the plasma cholesterol level when the hamsters are fed a chow diet and in susceptibility to diet-induced combined hyperlipidemia and coronary artery disease caused by the impaired clearance of circulating large lipoproteins. Moreover, homozygous *Ldlr* KO hamsters on the chow diet display severe hypercholesterolemia and develop spontaneous atherosclerosis, in which atherosclerosis is accelerated and premature death is elicited as a response to HCHF treatment. These findings suggest that *Ldlr* KO hamster can be an informative tool for both basic and translational research in human atherosclerosis.

Consistent with the FH patients with *Ldlr* gene mutations who have severe hypercholesterolemia in homozygous form and moderate hypercholesterolemia in heterozygous form, both the *Ldlr* −/− and *Ldlr* +/− hamsters exhibited severe and moderate forms, respectively, of hypercholesterolemia compared to the control animals. The homozygous form of the *Ldlr* gene deletion demonstrates various extents of hypercholesterolemia in many other species, including mice, rats, rabbits and pigs; however, the plasma cholesterol levels for the heterozygous form in these species are not elevated significantly (Ishibashi et al. 1993; Atkinson et al. 1989; Davis et al. 2014; Li et al. 2016). These findings suggest that hypercholesterolemia in hamsters with *Ldlr* ablation is an autosomal dominant disease and that *Ldlr* ablation has a gene-dosage effect on hypercholesterolemia, which has been well established in FH patients, indicating that targeted strategies based on studies of hamsters with different *Ldlr* defects are more valuable. However, in contrast to FH patients, the cholesterol concentration in the VLDL fraction is higher in chow diet-fed homozygous *Ldlr* KO hamsters than in humans. As CETP

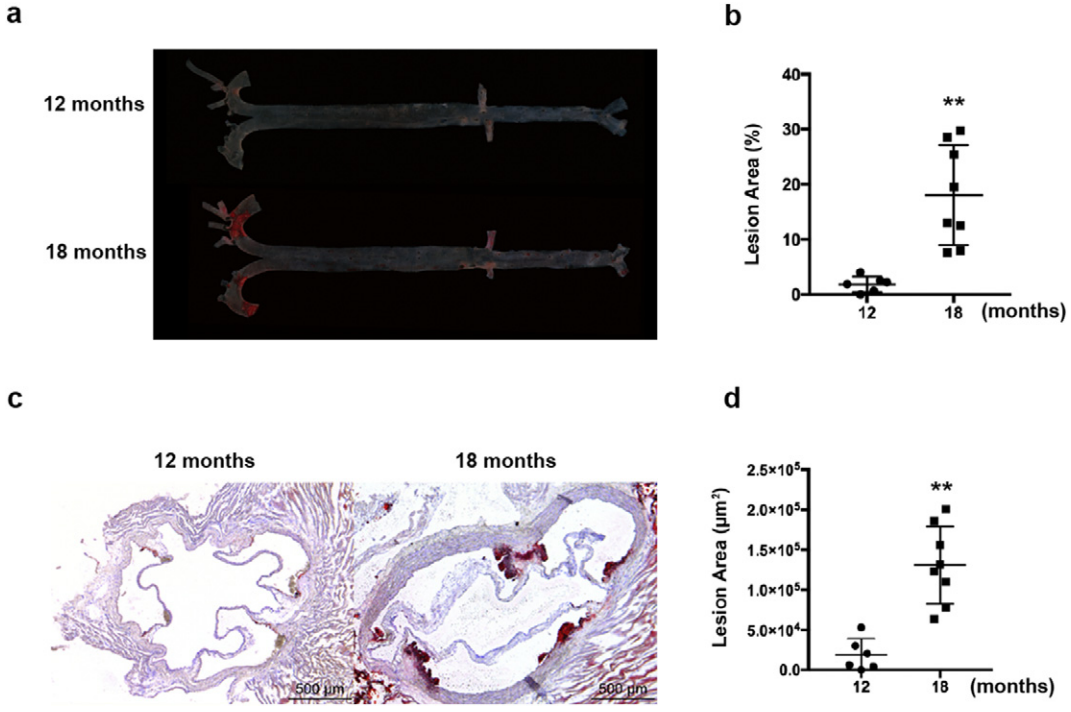

Fig. 5. Spontaneous atherosclerosis in *Ldlr* −/− hamsters on the chow diet. Atherosclerotic lesions were analyzed in male *Ldlr* −/− hamsters on a regular chow diet for 12 and 18 months. (a) Representative image en face. (b) Lesion areas were quantified (n = 8 per group). (c) Representative image of the sections from the aortic root. (d) Lesion areas were quantified (n = 8 per group). All data are expressed as the mean ± SEM. ** denotes $p < 0.01$.

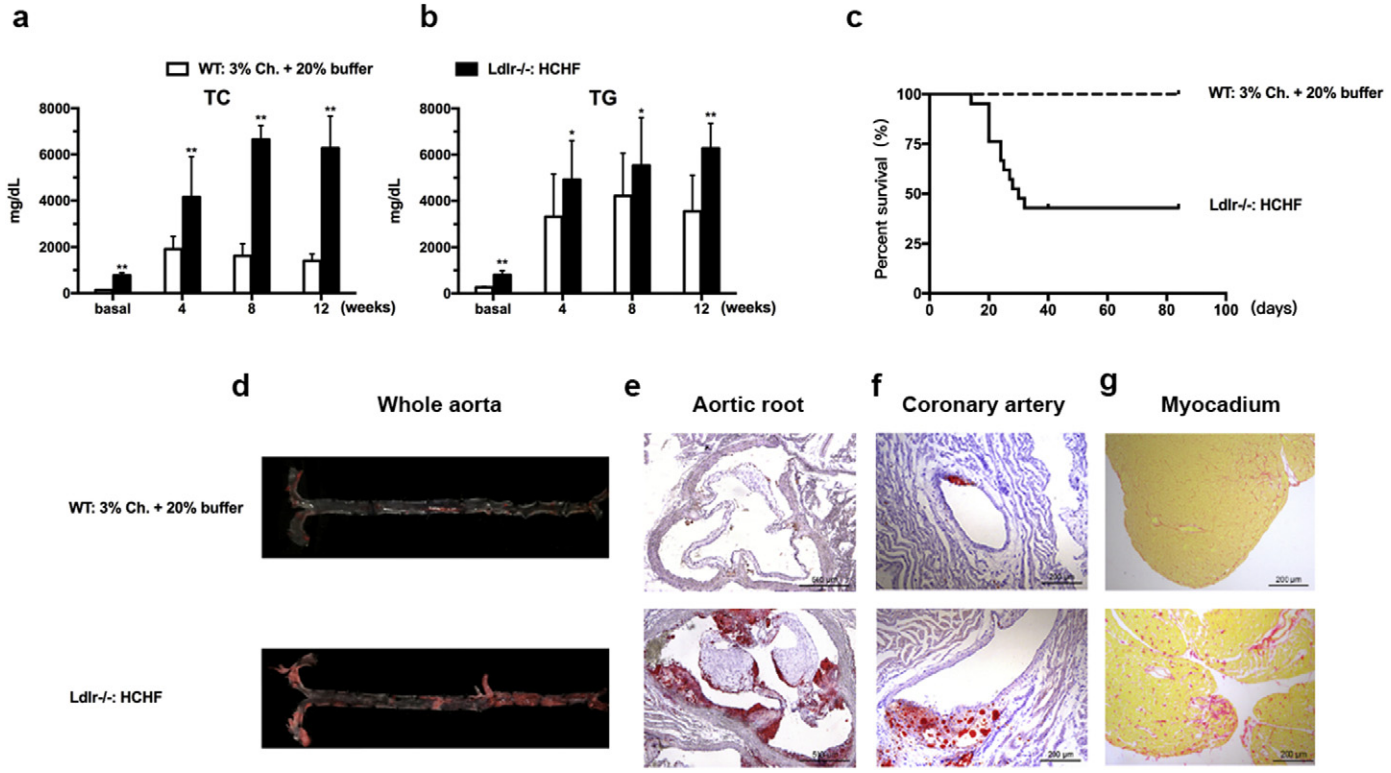

Fig. 6. HCHF-Induced Coronary Artery Disease in *Ldlr* −/− Hamsters. Male *Ldlr* −/− hamsters aged 8–10 weeks (n = 17) were fed the HCHF diet for 12 weeks. Sex-matched WT controls at the same age (n = 10) were on a special diet containing 3% cholesterol and 20% butter. (a and b) Plasma TC and TG. (c) Survival rate on the HCHF diet. (d-f) Oil Red O staining of the whole aorta, aortic root and coronary artery from the *Ldlr* −/− hamsters. (g) Sirius red staining of the myocardium from the WT and *Ldlr* −/− hamsters on the indicated diets. All data are expressed as the mean ± SEM. ** denotes $p < 0.01$.

is highly expressed in hamsters, in which the transfer capacity of TG to CE is highest compared to other species (Morton and Izem 2015), we speculate that the complete loss of *Ldlr* in the hamster can affect CETP expression and activity through unknown molecular mechanisms, leading to cholesterol accumulation in very large lipoproteins, such as VLDLs.

Unlike plasma total cholesterol, triglyceride levels are not altered in heterozygous hamsters but are significantly increased in homozygous animals. Since the rates of hepatic VLDL-TG secretion are identical in chow diet-fed hamsters, it is unlikely that VLDL-TG overproduction from the liver accounts for an increase in plasma TG. In addition, plasma LPL activity is also normal in *Ldlr* −/− hamsters, indicating that LPL can effectively hydrolyze very large TG-rich chylomicrons derived from the diet to form chylomicron remnants. Previously, Ishibashi et al. reported that chylomicron remnants were accumulated in *Ldlr* −/− mice and demonstrated a central role for the LDLR pathway in chylomicron remnant metabolism. Consistent with these findings, our results from the oral fat load experiment showed markedly increased TG levels in the *Ldlr*-ablated hamsters, suggesting that the accumulated TG-rich chylomicron remnants from LPL-mediated lipolysis could not be effectively removed via the LDLR pathway. Interestingly, the data of VLDL secretion demonstrated that *Ldlr* deficiency did not impair hepatic VLDL secretion in chow diet-fed hamsters; however, HCHF diet predisposed *Ldlr* −/− hamsters to severe hyperlipidemia, then probably leading to fatty liver to impair normal liver function, including VLDL secretion. More experiments will be needed to investigate the regulatory mechanisms underlying the pathogenesis of impaired VLDL secretion in *Ldlr* −/− hamsters after HCHF diet feeding.

Compared to homozygous FH (HoFH, prevalence 1:160,000–1,000,000), heterozygous FH (HeFH) is relatively common (prevalence 1:250–500). HeFH patients without treatments show a 20-fold increase in risk for cardiovascular heart disease (CHD), suggesting that not only HoFH but also HeFH needs diagnosis, monitoring and treatment (Cuchel et al. 2014). However, heterozygous *Ldlr*-mutant mice are resistant to diet-induced hyperlipidemia, making the use of this model difficult for studies of HeFH and its related symptoms. Although the Paigen diet (1.25% cholesterol with 0.5% cholate supplement) can elicit hypercholesterolemia in mice, this special diet is preferably avoided because the high concentration of dietary cholate is highly toxic to the liver and induces steatohepatitis in animals. In contrast to the findings in HCHF-fed *Ldlr* +/− mice, HCHF diet accelerated severe hypercholesterolemia in the *Ldlr* +/− hamsters. This significant discrepancy of diet-induced hypercholesterolemia between the mouse and hamster further confirmed the high similarities between hamsters and humans, suggesting that *Ldlr* +/− hamsters would be highly selective for assessing drug efficacy in the future. Statins are the drugs originally used for lowering the plasma cholesterol concentration, but accumulative evidence demonstrates that statins are not potent enough to reduce CHD risk and that conflicting outcomes have been observed in different clinical trials due to muscle-related side effects of these drugs (Lu et al. 2016; Wadhera et al. 2016; Dubroff and de Lorgeril 2015; Pursnani et al. 2015; Genest Jr et al. 1992). Recently, experimental data from animals have indicated that statins have anti-inflammatory activities and reduce the progression of atherosclerosis independently of their plasma cholesterol lowering effects (Kleemann et al. 2003). Moreover, Fenofibrate, an agonist of peroxisome proliferator-activated receptor alpha (PPAR alpha), has specifically been used to reduce triglyceride levels in patients with metabolic syndrome. Similar to Rosuvastatin, Fenofibrate also partially reduced both the TC and TG levels in the *Ldlr* +/− hamster with high cholesterol and high triglycerides after 2 weeks on the HCHF diet. This effectiveness of Fenofibrate in the *Ldlr* +/− hamster is clinically relevant to the advice that the combination of statin and fibrate is applicable for treating patients with combined hyperlipidemia. Hereby, our findings suggest that a promising therapeutic strategy for FH should be considered.

A buildup of atherosclerotic plaque in the coronary and carotid arteries is the endpoint consequence of FH (Goldstein et al. 1983). Although

Ldlr −/− and *Apoe* −/− mice exhibit atherogenic lesion development and are extensively used for studying atherosclerosis, these 2 models rarely develop clinically relevant coronary artery atherosclerosis without any special genetic or environmental manipulation (Getz and Reardon 2016). Importantly, the loss of one copy of *Ldlr* in mice does not cause marked alterations in plasma lipids. Thus, the heterozygous forms of *Ldlr*- and *Apoe*-ablated mice have not been used for atherogenic studies (Ishibashi et al. 1993). Rationally, the possibility to investigate atherosclerotic development is one of the important features of our animal models. In our present study, the *Ldlr* +/− hamsters showed severe hypercholesterolemia beginning at 2 weeks after being fed the HCHF diet to the experimental endpoint and accelerated atherosclerotic plaque found in different segments, which were not affected by the sex. In the clinical studies, the conclusions of sex effect on atherosclerosis in FH patients are controversial; however, a HuGE association study has revealed that different ethnicities contribute to diverse associations between FH and CHD (Austin et al. 2004), suggesting that sex is not a critical determinant of atherosclerotic development using animal models for FH study. This valuable information from the HCHF-fed *Ldlr* +/− hamsters provides strong evidence for the use of a different animal model that potentially mimics CHD in FH patients.

It is to be noted that hamsters display similar lipoprotein profiles and coronary atherosclerosis to those observed in FH patients, however, our present study leaves some unanswered questions. 1) Since hamsters have high plasma CETP activity and the CETP inhibitor Anacetrapib was recently shown to significantly reduce major coronary events (Group et al. 2017), do *Ldlr*-ablated hamsters respond to Anacetrapib treatment and whether CETP inhibition would be effective to lower VLDL cholesterol in our model? 2) Given the marked reduction in TC in the HCHF-fed *Ldlr* +/− hamsters by Ezetimibe, which acts by decreasing cholesterol absorption in the small intestine, does lowering dietary cholesterol contribute to the improved lipoprotein profile and consequent outcome of coronary disease in HCHF-fed *Ldlr*-ablated hamsters? In the future, it is tempting to use our special hamster model to solve these issues and provide insights into translational research of human atherosclerosis.

In conclusion, our results demonstrate that *Ldlr*-mutant hamsters display special advantages over other species in terms of autosomal dominant inheritance, plasma lipid metabolism and the development of coronary atherosclerotic lesions. Advantages also include the easy breeding of hamsters with a short pregnancy term (17 days) and large litter size (~12 per litter), and thus, *Ldlr*-ablated hamsters will definitely serve as an ideal platform over other small animal models for basic and translational research of dyslipidemia and atherosclerosis.

Conflicts of Interest

The authors declare that they have no competing interests. There are no relationships with the industry.

Authors' Contributions

Y.W., L.Y., G.L. and X.X. conceived and designed the study. X.G., M.G., Y.W., X.L., J.W., B.A. and N.C. performed the experiments. X.G., M.G., and Y.W. collected and analyzed the data. L.Y., F.W., K.Q., L.Y., Y.W., H.Z., G.L. and X.X. interpreted the data. X.G., L.Y., G.L. and X.X. wrote the paper. Y.W. and G.L. acquired the funding. G.L. and X.X. supervised the study. G.L. and X.X. reviewed and edited the manuscript.

Acknowledgements and Funding Sources

This work is financially supported in part by a collaborative grant from the Center for Molecular and Translational Medicine (BMU20140475), by the National Natural Science Foundation of China (31520103909 and 81270367) to GL and by a National Natural Science Foundation of China (NSFC) - 81570787 to YW. GL is a fellow at the Collaborative Innovation Center for Cardiovascular Disease Translational Medicine, Nanjing Medical University.

Appendix A. Supplementary data

Supplementary data to this article can be found online at https://doi.org/10.1016/j.ebiom.2017.12.013.

References

Atkinson, J.B., Hoover, R.L., Berry, K.K., Swift, L.L., 1989. Cholesterol-fed heterozygous Watanabe heritable hyperlipidemic rabbits: a new model for atherosclerosis. Atherosclerosis 78, 123–136.

Austin, M.A., Hutter, C.M., Zimmern, R.L., Humphries, S.E., 2004. Familial hypercholesterolemia and coronary heart disease: a HuGE association review. Am. J. Epidemiol. 160, 421–429.

Bjorklund, M.M., Hollensen, A.K., Hagensen, M.K., Dagnaes-Hansen, F., Christoffersen, C., Mikkelsen, J.G., Bentzon, J.F., 2014. Induction of atherosclerosis in mice and hamsters without germline genetic engineering. Circ. Res. 114, 1684–1689.

Cong, L., Ran, F.A., Cox, D., Lin, S., Barretto, R., Habib, N., Hsu, P.D., Wu, X., Jiang, W., Marraffini, L.A., Zhang, F., 2013. Multiplex genome engineering using CRISPR/Cas systems. Science 339, 819–823.

Cuchel, M., Bruckert, E., Ginsberg, H.N., Raal, F.J., Santos, R.D., Hegele, R.A., Kuivenhoven, J.A., Nordestgaard, B.G., Descamps, O.S., Steinhagen-Thiessen, E., Tybjaerg-Hansen, A., Watts, G.F., Averna, M., Boileau, C., Boren, J., Catapano, A.L., Defesche, J.C., Hovingh, G.K., Humphries, S.E., Kovanen, P.T., Masana, L., Pajukanta, P., Parhofer, K.G., Ray, K.K., Stalenhoef, A.F., Stroes, E., Taskinen, M.R., Wiegman, A., Wiklund, O., Chapman, M.J., European Atherosclerosis Society Consensus Panel on Familial, H, 2014. Homozygous familial hypercholesterolaemia: new insights and guidance for clinicians to improve detection and clinical management. A position paper from the Consensus panel on familial Hypercholesterolaemia of the European atherosclerosis Society. Eur. Heart J. 35, 2146–2157.

Davis, B.T., Wang, X.J., Rohret, J.A., Struzynski, J.T., Merricks, E.P., Bellinger, D.A., Rohret, F.A., Nichols, T.C., Rogers, C.S., 2014. Targeted disruption of LDLR causes hypercholesterolemia and atherosclerosis in Yucatan miniature pigs. PLoS One 9, e93457.

DI Filippo, M., Marcais, C., Charriere, S., Marmontel, O., Broyer, M., Delay, M., Merlin, M., Nollace, A., Valero, R., Lagarde, M., Pruneta-Deloche, V., Moulin, P., Sassolas, A., 2014. Post-heparin LPL activity measurement using VLDL as a substrate: a new robust method for routine assessment of plasma triglyceride lipolysis defects. PLoS One 9, e99721.

Dubroff, R., de Lorgeril, M., 2015. Cholesterol confusion and statin controversy. World J. Cardiol. 7, 404–409.

Fan, Z., Li, W., Lee, S.R., Meng, Q., Shi, B., Bunch, T.D., White, K.L., Kong, I.K., Wang, Z., 2014. Efficient gene targeting in golden Syrian hamsters by the CRISPR/Cas9 system. PLoS One 9, e109755.

Gao, M., Zhang, B., Liu, J., Guo, X., Li, H., Wang, T., Zhang, Z., Liao, J., Cong, N., Wang, Y., Yu, L., Zhao, D., Liu, G., 2014. Generation of transgenic golden Syrian hamsters. Cell Res. 24, 380–382.

Genest Jr., J.J., Martin-Munley, S.S., McNamara, J.R., Ordovas, J.M., Jenner, J., Myers, R.H., Silberman, S.R., Wilson, P.W., Salem, D.N., Schaefer, E.J., 1992. Familial lipoprotein disorders in patients with premature coronary artery disease. Circulation 85, 2025–2033.

Getz, G.S., Reardon, C.A., 2006. Diet and murine atherosclerosis. Arterioscler. Thromb. Vasc. Biol. 26, 242–249.

Getz, G.S., Reardon, C.A., 2016. Do the Apoe −/− and Ldlr −/− mice yield the same insight on Atherogenesis? Arterioscler. Thromb. Vasc. Biol. 36, 1734–1741.

Goldstein, J.L., Kita, T., Brown, M.S., 1983. Defective lipoprotein receptors and atherosclerosis. Lessons from an animal counterpart of familial hypercholesterolemia. N. Engl. J. Med. 309, 288–296.

Group, H. T. R. C, Bowman, L., Hopewell, J.C., Chen, F., Wallendszus, K., Stevens, W., Collins, R., Wiviott, S.D., Cannon, C.P., Braunwald, E., Sammons, E., Landray, M.J., 2017. Effects of Anacetrapib in patients with atherosclerotic vascular disease. N. Engl. J. Med. 377, 1217–1227.

Haidari, M., Leung, N., Mahbub, F., Uffelman, K.D., Kohen-Avramoglu, R., Lewis, G.F., Adeli, K., 2002. Fasting and postprandial overproduction of intestinally derived lipoproteins in an animal model of insulin resistance. Evidence that chronic fructose feeding in the hamster is accompanied by enhanced intestinal de novo lipogenesis and ApoB48-containing lipoprotein overproduction. J. Biol. Chem. 277, 31646–31655.

Hobbs, H.H., Brown, M.S., Goldstein, J.L., 1992. Molecular genetics of the LDL receptor gene in familial hypercholesterolemia. Hum. Mutat. 1, 445–466.

Ishibashi, S., Brown, M.S., Goldstein, J.L., Gerard, R.D., Hammer, R.E., Herz, J., 1993. Hypercholesterolemia in low density lipoprotein receptor knockout mice and its reversal by adenovirus-mediated gene delivery. J. Clin. Invest. 92, 883–893.

Kleemann, R., Princen, H.M., Emeis, J.J., Jukema, J.W., Fontijn, R.D., Horrevoets, A.J., Kooistra, T., Havekes, L.M., 2003. Rosuvastatin reduces atherosclerosis development beyond and independent of its plasma cholesterol-lowering effect in APOE*3-Leiden transgenic mice: evidence for antiinflammatory effects of rosuvastatin. Circulation 108, 1368–1374.

Li, Y., Fuchimoto, D., Sudo, M., Haruta, H., Lin, Q.F., Takayama, T., Morita, S., Nochi, T., Suzuki, S., Sembon, S., Nakai, M., Kojima, M., Iwamoto, M., Hashimoto, M., Yoda, S., Kunimoto, S., Hiro, T., Matsumoto, T., Mitsumata, M., Sugitani, M., Saito, S., Hirayama, A., Onishi, A., 2016. Development of human-like advanced coronary

plaques in low-density lipoprotein receptor knockout pigs and justification for statin treatment before formation of atherosclerotic plaques. J. Am. Heart Assoc. 5, e002779.
Lu, Y., Cheng, Z., Zhao, Y., Chang, X., Chan, C., Bai, Y., Cheng, N., 2016. Efficacy and safety of long-term treatment with statins for coronary heart disease: a Bayesian network meta-analysis. Atherosclerosis 254, 215–227.
Millar, J.S., Cromley, D.A., McCoy, M.G., Rader, D.J., Billheimer, J.T., 2005. Determining hepatic triglyceride production in mice: comparison of poloxamer 407 with Triton WR-1339. J. Lipid Res. 46, 2023–2028.
Morton, R.E., Izem, L., 2015. Modification of CETP function by changing its substrate preference: a new paradigm for CETP drug design. J. Lipid Res. 56, 612–619.
Pasterkamp, G., van der Laan, S.W., Haitjema, S., Foroughi ASL, H., Siemelink, M.A., Bezemer, T., van Setten, J., Dichgans, M., Malik, R., Worrall, B.B., Schunkert, H., Samani, N.J., de Kleijn, D.P., Markus, H.S., Hoefer, I.E., Michoel, T., de Jager, S.C., Bjorkegren, J.L., den Ruijter, H.M., Asselbergs, F.W., 2016. Human validation of genes associated with a murine atherosclerotic phenotype. Arterioscler. Thromb. Vasc. Biol. 36, 1240–1246.
Pursnani, A., Massaro, J.M., D'agostino Sr., R.B., O'donnell, C.J., Hoffmann, U., 2015. Guideline-based statin eligibility, coronary artery calcification, and cardiovascular events. JAMA 314, 134–141.
Reaves, S.K., Wu, J.Y., Wu, Y., Fanzo, J.C., Wang, Y.R., Lei, P.P., Lei, K.Y., 2000. Regulation of intestinal apolipoprotein B mRNA editing levels by a zinc-deficient diet and cDNA cloning of editing protein in hamsters. J. Nutr. 130, 2166–2173.
Sima, A., Bulla, A., Simionescu, N., 1990. Experimental obstructive coronary atherosclerosis in the hyperlipidemic hamster. J. Submicrosc. Cytol. Pathol. 22, 1–16.
Wadhera, R.K., Steen, D.L., Khan, I., Giugliano, R.P., Foody, J.M., 2016. A review of low-density lipoprotein cholesterol, treatment strategies, and its impact on cardiovascular disease morbidity and mortality. J. Clin. Lipidol. 10, 472–489.